

Limit of Spin Squeezing in Finite Temperature Bose-Einstein Condensates

A. Sinatra,¹ E. Witkowska,² J.-C. Dornstetter,¹ Li Yun,¹ and Y. Castin¹

¹Laboratoire Kastler Brossel, Ecole Normale Supérieure, UPMC and CNRS, Paris, France

²Institute of Physics, Polish Academy of Sciences, Warszawa, Poland

We show that, at finite temperature, the maximum spin squeezing achievable using interactions in Bose-Einstein condensates has a finite limit when the atom number $N \rightarrow \infty$ at fixed density and interaction strength. We calculate the limit of the squeezing parameter for a spatially homogeneous system and show that it is bounded from above by the initial non-condensed fraction.

PACS numbers: 03.75.Gg, 42.50.Dv, 03.75.Kk, 03.75.Pp, 03.75.Mn.

Atomic clocks based on cold alkali atoms in two hyperfine states a and b are widely used as frequency standards. When atoms in uncorrelated quantum states are used, the clock precision is limited by the so-called projection noise, resulting from the quantum nature of the collective spin \mathbf{S} , *i.e.* the sum of the effective spin $1/2$ of each atom. This limit is actually already reached in most precise clocks [1]. Spin squeezing [2] amounts to creating quantum correlations among the atoms so as to increase the precision of the atomic clock beyond this standard quantum limit. The relative improvement on the variance of the measured frequency $\Delta\omega_{ab}^2$ defines the spin squeezing parameter ξ^2 [3]. Spin squeezing in atomic ensembles was first obtained by quantum non-demolition measurements [4, 5]. Recently a significant amount of spin squeezing (e.g. 6 or 8 dB) has been achieved using atoms in a resonant optical cavity [6] or exploiting atomic interactions in bimodal Bose-Einstein condensates [7–9]. The ultimate limits of the different paths to spin squeezing are still an open question. We determine here the influence of the non-condensed fraction for spin squeezing schemes using Bose-Einstein condensates [8–10].

A central issue is the *scaling of the squeezing* for large atom numbers. Most studies are based on a two-mode description [2]. In this case the squeezing parameter optimized over time ξ_{best}^2 tends to zero (infinite metrology gain) for $N \rightarrow \infty$ as $\xi_{\text{best}}^2 \sim N^{-2/3}$. The first analysis of squeezing at finite temperature [11] used a large N expansion in a Bogoliubov-like approach and could not predict any deviation of spin squeezing from the two-mode model. Here, using fully non-perturbative semi-classical field simulations and a powerful formulation of Bogoliubov theory in terms of the time dependent condensate phase operator [12], we find on the contrary a dramatic effect of the multimode nature of the field: For a spatially homogeneous system in the thermodynamic limit, the two-mode scaling $\xi_{\text{best}}^2 \sim N^{-2/3}$ turns out to be completely irrelevant, and the spin squeezing has a finite optimal value that we determine analytically.

The physical problem that we face is the dynamical evolution of a finite temperature Bose condensed gas after a pulse $\pi/2$ that puts each atom in a coherent superposition of two internal states a and b . This produces a

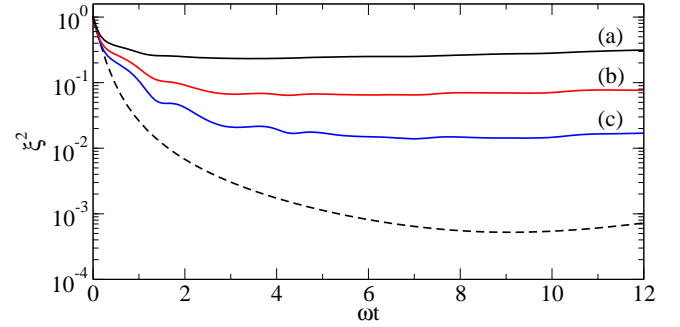


FIG. 1: (Color online) Spin squeezing parameter ξ^2 as a function of time after the pulse mixing the states a and b , for $N = 10^5$ Rb atoms (s -wave scattering length $a = 5.3$ nm), in a harmonic trap with oscillation frequency $\omega/2\pi = 50$ Hz. The Thomas-Fermi chemical potential is $\mu = 15.36\hbar\omega$. Finite temperature semi-classical field simulations with initial non-condensed fractions: (a) $\langle N_{\text{nc}} \rangle / N = 0.34$ (black solid line), (b) $\langle N_{\text{nc}} \rangle / N = 0.20$ (red line), (c) $\langle N_{\text{nc}} \rangle / N = 0.09$ (blue line), corresponding to $k_B T / \mu = 2.08, 1.53, 1.17$ respectively. Dashed line: Two-mode theory for comparison.

non-equilibrium state that has a non-trivial evolution due to the atomic interactions inside each internal state. For simplicity, it is assumed that there is no cross-interaction between a and b atoms.

Semi-classical field simulations - In Fig.1 we compare the two-mode theory with semi-classical field simulations at finite temperature in a trap. The gas is initially in state a at thermal equilibrium. In that state, we assume that thermal fluctuations dominate over quantum fluctuations and we use a classical field description [13–16] with an energy cut-off at $k_B T$. The initial field $\psi_a^{(0)}$ then randomly samples the thermal equilibrium classical field distribution for the canonical ensemble at temperature T . For the initially empty state b , inspired by the truncated Wigner approach [17, 18] we represent the vacuum by a classical field $\psi_b^{(0)}$ having in each mode independent Gaussian complex fluctuations of zero mean and variance $1/2$. A sudden $\pi/2$ pulse mixes the initial fields $\psi_a^{(0)}$ and $\psi_b^{(0)}$ so that, at time $t = 0^+$, *i.e.* just after the pulse:

$$\psi_{a,b}(0^+) = \frac{1}{\sqrt{2}}[\psi_{a,b}^{(0)} \mp \psi_{b,a}^{(0)}]. \quad (1)$$

At later times, each field evolves independently according to the non-linear Schrödinger equation

$$i\hbar \partial_t \psi_{a,b} = \left[-\frac{\hbar^2 \Delta}{2m} + \frac{1}{2} m \omega^2 \mathbf{r}^2 + g |\psi_{a,b}(\mathbf{r}, t)|^2 \right] \psi_{a,b}. \quad (2)$$

This corresponds to a harmonically trapped gas with same oscillation frequency ω and same coupling constant $g = 4\pi\hbar^2 a/m$ for the two internal states, where a is the s -wave scattering length. As shown in Fig.1, the squeezing is created dynamically by the interactions. However, even for a moderate non-condensed fraction $\langle N_{nc} \rangle / N = 0.09$, the best ξ^2 in the multimode theory is larger by more than one order of magnitude than in the two-mode theory.

In order to isolate the effect of the non-condensed fraction from other dynamical effects taking place in the trapped system, as for example the spatial dynamics of the condensate wave function [19, 20], and to develop an analytical theory, we consider from now-on the homogeneous case. We first use the semi-classical field model that has the advantage that it can be simulated exactly, and we generalize the results to the case of a quantum field in the end. The real space is discretized on a lattice with unit cell of volume dV , within a volume V with periodic boundary conditions [12]. The Hamiltonian after the pulse for component a (and similarly for b) reads:

$$H = \sum_{\mathbf{k}} \frac{\hbar^2 k^2}{2m} a_{\mathbf{k}}^* a_{\mathbf{k}} + \frac{g}{2} dV \sum_{\mathbf{r}} |\psi_a(\mathbf{r})|^4. \quad (3)$$

The fields have Poisson brackets $i\hbar \{ \psi_\mu(\mathbf{r}), \psi_\nu^*(\mathbf{r}') \} = \delta_{\mathbf{r}\mathbf{r}'} \delta_{\mu\nu} / dV$ with $\mu, \nu = a$ or b , and $a_{\mathbf{k}}(b_{\mathbf{k}})$ is the amplitude of $\psi_{a(b)}$ the over the plane wave of momentum \mathbf{k} . In terms of the fields, the collective spin components are

$$S_x + iS_y = \int d^3\mathbf{r} \psi_a^*(\mathbf{r}) \psi_b(\mathbf{r}), \quad (4)$$

$$S_z = \frac{1}{2} \int d^3\mathbf{r} [\psi_a^*(\mathbf{r}) \psi_a(\mathbf{r}) - \psi_b^*(\mathbf{r}) \psi_b(\mathbf{r})]. \quad (5)$$

The spin squeezing parameter ξ^2 is equivalent to the minimal variance of the spin orthogonally to its mean direction, divided by the mean spin length squared and suitably normalized. Here the mean spin is along x so that

$$\xi^2(t) = \frac{\Delta S_{\perp, \min}^2(t)}{\langle S_x(t) \rangle^2} \times \frac{\langle S_x(0^+) \rangle^2}{\Delta S_{\perp, \min}^2(0^+)} \quad (6)$$

$$\Delta S_{\perp, \min}^2 = \frac{1}{2} [\langle S_y^2 \rangle + \langle S_z^2 \rangle - | \langle (S_y + iS_z)^2 \rangle |]. \quad (7)$$

As a first step, we performed semi-classical field simulations for different temperatures and increasing system sizes [21]. The result (not shown) is that ξ_{best}^2 converges to a finite value at the thermodynamic limit: $N \rightarrow \infty$, $V \rightarrow \infty$, $\rho, g, T = \text{constant}$, where $\rho = N/V$ is the total density. Five independent physical parameters are in

the model, $\hbar/m, g$ or $a, k_B T, N$ and V . From dimensional analysis, ξ_{best}^2 is a function of the three independent dimensionless quantities that one can form, $N, \sqrt{\rho a^3}$, and $k_B T / \rho g$. The existence of a thermodynamic limit then implies

$$\xi_{\text{best}}^2 = f \left(\sqrt{\rho a^3}, \frac{k_B T}{\rho g} \right). \quad (8)$$

As a second step, we performed simulations increasing the density in the weakly interacting limit [22], $\rho \rightarrow \infty$, $g \rightarrow 0$ with $T, \rho g = \text{constant}$. We find that, for a given $k_B T / \rho g$, ξ_{best}^2 then scales as $1/\rho \propto \sqrt{\rho a^3}$. This implies:

$$\xi_{\text{best}}^2 / \sqrt{\rho a^3} = F(k_B T / \rho g). \quad (9)$$

In Fig.2 we show the universal behavior (9). The circles and the squares correspond to two different values of $\sqrt{\rho a^3}$ in simulations.

Semi-classical field analytics - We now develop an analytical theory to explain these results. We split the fields after the pulse as $\psi_a = \frac{a_0}{\sqrt{V}} + \psi_{a\perp}$ and similarly for ψ_b . We introduce the modulus and phase conjugate variables for the condensate modes

$$a_0 = e^{i\theta_a} \sqrt{N_{a0}}, \quad b_0 = e^{i\theta_b} \sqrt{N_{b0}}, \quad (10)$$

and we introduce number conserving non-condensed fields Λ_a and Λ_b [22] that we expand over Bogoliubov modes with amplitudes $c_{a\mathbf{k}}$ and $c_{b\mathbf{k}}$ respectively [23]:

$$\Lambda_a = e^{-i\theta_a} \psi_{a\perp} = \sum_{\mathbf{k} \neq 0} (U_k c_{a\mathbf{k}} + V_k c_{a-\mathbf{k}}^*) \frac{e^{i\mathbf{k} \cdot \mathbf{r}}}{\sqrt{V}} \quad (11)$$

$$U_k + V_k = \left(\frac{E_k}{E_k + \rho g} \right)^{1/4}; \quad E_k = \frac{\hbar^2 k^2}{2m}. \quad (12)$$

The spin raising component $S_+ = S_x + iS_y$ is given by

$$S_+ = e^{-i(\theta_a - \theta_b)} \left(\sqrt{N_{a0} N_{b0}} + \int d^3\mathbf{r} \Lambda_a^* \Lambda_b \right). \quad (13)$$

Our strategy is to perform a *double expansion* of $\langle S_+^2 \rangle$. We will need terms up to $\sim N$ in the thermodynamic limit and up to order one in the non-condensed fraction $\langle N_{nc} \rangle / N$. In this framework, we can approximate $\langle S_x(t) \rangle$ in the denominator of (7) by its value at $t = 0^+$ so that

$$\xi^2 \simeq \frac{4}{N} \Delta S_{\perp, \min}^2. \quad (14)$$

We sketch the main steps. In the Bogoliubov limit, the condensate phases at $t > 0$ obey [12]

$$\theta_a - \theta_b = (\theta_a - \theta_b)(0^+) - \frac{\rho g}{V} t [(N_a - N_b) + S] \quad (15)$$

$$(\theta_a - \theta_b)(0^+) = -2 \frac{\text{Im} b_0^{(0)}}{\sqrt{N_{a0}^{(0)}}} + O(N^{-1}) \quad (16)$$

$$S = \sum_{\mathbf{k} \neq 0} (U_k + V_k)^2 (|c_{a\mathbf{k}}|^2 - |c_{b\mathbf{k}}|^2). \quad (17)$$

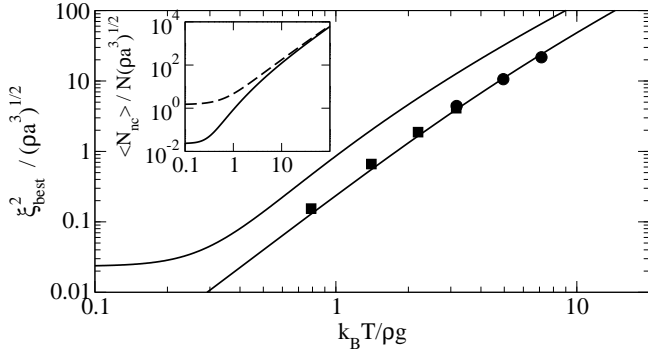


FIG. 2: Best squeezing ξ_{best}^2 divided by $\sqrt{\rho a^3}$ as a function of $k_B T / \rho g$. Symbols: semi-classical field simulations with $\sqrt{\rho a^3} = 1.32 \times 10^{-2}$ (filled squares) and 1.94×10^{-3} (disks). The thermodynamic limit is reached already for $N = 3 \times 10^4$ except for the lowest value of $k_B T / \rho g$. Lower solid line: analytical semi-classical field result (21). Upper solid line: quantum result (25). Inset: quantum ξ_{best}^2 (solid line) and non-condensed fraction $\langle N_{\text{nc}} \rangle / N$ (dashed line), both divided by $\sqrt{\rho a^3}$, as functions of $k_B T / \rho g$.

S is the *multimode part* of the relative phase derivative that is absent in the two-mode theory. In thermodynamic limit $\theta_a - \theta_b \sim 1/\sqrt{N}$ and it is sufficient to expand the exponential in (13) to second order. In the modulus of S_+ we expand:

$$\sqrt{N_{a0} N_{b0}} \simeq \frac{N_{\text{tot}}}{2} - \frac{1}{2} \int d^3 \mathbf{r} (|\Lambda_a|^2 + |\Lambda_b|^2) \quad (18)$$

with $N_{\text{tot}} = N + \sum_{\mathbf{k}} |b_{\mathbf{k}}^{(0)}|^2$ is the total atom number in the semi-classical field picture.

Best squeezing - For the calculation of the best squeezing, one looks at the asymptotic behavior of (14) for $t \rightarrow \infty$. One finds:

$$\xi^2(t) = \xi_{\text{best}}^2 + \left(\frac{\hbar}{\rho g t} \right)^2 \left[1 + O\left(\frac{\langle N_{\text{nc}} \rangle}{N} \right) \right] + O\left(\frac{1}{t^4} \right) \quad (19)$$

with the best squeezing

$$\xi_{\text{best}}^2 = \langle S^2 \rangle / N. \quad (20)$$

which remarkably only involves the multimode part (17) of the phase difference. An explicit calculation gives

$$\xi_{\text{best}}^2 = \frac{1}{2\rho} \int \frac{d^3 \mathbf{k}}{(2\pi)^3} s_k^4 n_k^{(0)} \left[\left(\frac{s_k^{(0)}}{s_k} \right)^2 + \left(\frac{s_k^2}{s_k^{(0)}} \right)^2 \right] \quad (21)$$

(solid line in Fig.2). In (21), $s_k = U_k + V_k$ given in (12), and $s_k^{(0)}$ is the equivalent quantity before the pulse obtained by replacing ρg with $2\rho g$ in (12); $n_k^{(0)} = k_B T / \epsilon_k^{(0)}$ are the equilibrium occupation numbers of Bogoliubov modes before the pulse with $\epsilon_k^{(0)} = [E_k(E_k + 2\rho g)]^{1/2}$.

Squeezing time - From (19), the best squeezing is reached in an infinite time, which is a limitation of the

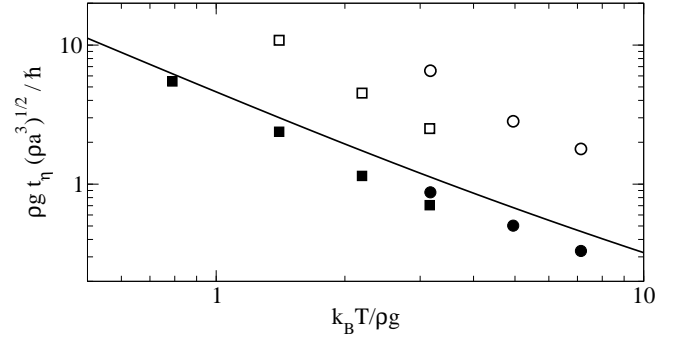


FIG. 3: “Close to best” squeezing time t_η for $\eta = 0.2$. Filled squares and disks: simulations as in Fig.2. Line: analytical prediction (22). Squares and circles: thermalization times in the simulations extracted from the decay of the contrast $\langle S_x \rangle$.

analytical approach. However, the numerical squeezing curve as a function of time is indeed quite flat around its minimum, so that it suffices in practice to determine the “close to best” squeezing time t_η defined as $\xi^2(t_\eta) = (1 + \eta)\xi_{\text{best}}^2$, where $\eta > 0$. Then, according to (19), t_η is finite and given by

$$\frac{\rho g}{\hbar} t_\eta = \frac{1}{\sqrt{\eta \xi_{\text{best}}^2}}. \quad (22)$$

The “close to best” squeezing time t_η (22) for $\eta = 0.2$ is shown in Fig.3 and compared to simulations.

A last important issue is that of *thermalization*, neglected in Bogoliubov theory and in our analytical treatment, but fully included in the semi-classical field simulations. Indeed it is possible to reach $\xi^2 = (1 + \eta)\xi_{\text{best}}^2$ with ξ_{best}^2 given by (21) only if t_η given by (22) is shorter than the thermalization time

$$t_\eta < t_{\text{therm}}. \quad (23)$$

In Fig.4 we show the squeezing parameter ξ^2 and contrast $\langle S_x \rangle$ across the thermalization process that brings the system back to equilibrium after the pulse. For the squeezing, we compare the simulation with (i) the full Bogoliubov theory (without the analytic expansions) that we implement numerically for a finite size system and (ii) a Bogoliubov ergodic model [12] where the amplitudes $c_{a\mathbf{k}}$, $c_{b\mathbf{k}}$ in (15) sample microcanonical distributions with number of particles and the energy $\{N_a, E_a\}$ ($\{N_b, E_b\}$) fixed to a random value set by the pulse. Note that the simulation agrees with the Bogoliubov model at short times (included the “close to best” squeezing time) and then converges towards the ergodic model. We extract a thermalization time t_{therm} from the contrast. As thermalization occurs the excited modes dephase and

$$\langle S_x \rangle = \text{Re} \left(\sum_{\mathbf{k}} b_{\mathbf{k}}^* a_{\mathbf{k}} \right) \Big|_{t \rightarrow \infty} \sim \text{Re}(b_0^* a_0). \quad (24)$$

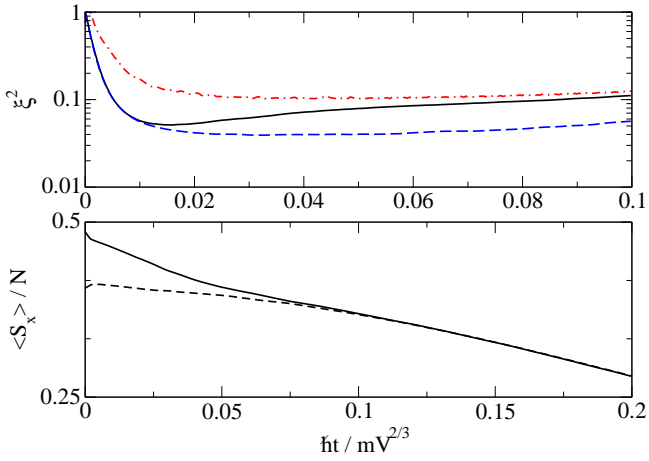


FIG. 4: (Color online) Top: Spin squeezing ξ^2 as a function of time. Black solid line: simulation. Blue dashed line: Bogoliubov theory. Red dash-dotted line: ergodic model. Bottom: contrast $\langle S_x \rangle$ (solid line) and condensate contrast $\text{Re}\langle b_0^* a_0 \rangle$ (dashed line) as functions of time. $N = 3 \times 10^4$, $k_B T / \rho g = 3.16$, $\sqrt{\rho a^3} = 1.32 \times 10^{-2}$.

The longer time scale for the decay of $\langle b_0^* a_0 \rangle$ is set by phase spreading due to partition noise [24] plus thermal corrections.

Quantum field - All our analytic calculations for the semi-classical field can be generalized to the quantum field. In particular, (20) and (22) are unchanged and

$$\xi_{\text{best}}^2 = \int \frac{d^3 \mathbf{k}}{(2\pi)^3} \frac{s_k^4}{2\rho} \left[\left(n_k^{(0)} + \frac{1}{2} \right) \left(\frac{(s_k^{(0)})^2}{s_k^4} + \frac{s_k^4}{(s_k^{(0)})^2} \right) - 1 \right]. \quad (25)$$

At zero temperature we get

$$\frac{\xi_{\text{best}}^{2T=0}}{\sqrt{\rho a^3}} = \sqrt{\frac{8}{\pi}} \left[\frac{19}{6} \sqrt{2} - \frac{3}{2} \ln(\sqrt{2} + 1) - \pi \right] \simeq 0.02344. \quad (26)$$

In practice $\rho a^3 < 10^{-6}$ in present squeezing experiments so that (26) predicts $\xi_{\text{best}}^{2T=0} \lesssim 2.10^{-5}$. This value is very low, in particular below the limit given by particle losses [25]. Asymptotically for $k_B T \gg \rho g$, ξ_{best}^2 identifies with the initial non-condensed fraction. An interesting result is that at any temperature the initial non-condensed fraction is larger than ξ_{best}^2 , see these two quantities in the inset of Fig.2. Already for $k_B T / \rho g = 2$, ξ_{best}^2 and $\langle N_{\text{nc}} \rangle / N$ are within a factor three. A similar conclusion seems to hold in a trap, see Fig.1.

In conclusion we have shown that a realistic description of the limits of spin squeezing in interacting Bose-Einstein condensates has to be multimode: The best achievable spin squeezing ξ_{best}^2 admits a finite limit for

$N \rightarrow \infty$ at fixed density and interaction strength, contrarily to the vanishing prediction of the two-mode model. We find that ξ_{best}^2 is the product of $\sqrt{\rho a^3}$ and of a universal function of $k_B T / \rho g$ that we calculated analytically, and is bounded from above by the initial non-condensed fraction. Our analytical treatment is restricted to evolution times smaller than the thermalization time, but this is enough to access ξ_{best}^2 as we showed by semi-classical field simulations (that include thermalization) over a wide range of parameters.

EW acknowledges support from Polish Government Research Funds: N N202 104136, 2009-2011.

-
- [1] G. Santarelli et al., Phys. Rev. Lett. **82**, 4619 (1999).
 - [2] M. Kitagawa and M. Ueda, Phys. Rev. A **47**, 5138 (1993).
 - [3] D. J. Wineland et al., Phys. Rev. A **50**, 67 (1994).
 - [4] A. Kuzmich, L. Mandel, and N. P. Bigelow, Phys. Rev. Lett. **85**, 1594 (2000).
 - [5] A. Louchet-Chauvet et al., New Journal of Physics **12**, 065032 (2010).
 - [6] Ian D. Leroux et al., Phys. Rev. Lett. **104**, 073602 (2010).
 - [7] J. Estève et al., Nature **455**, 1216 (2008).
 - [8] C. Gross et al., Nature **464**, 1165 (2010).
 - [9] M. F. Riedel et al., Nature **464**, 1170 (2010).
 - [10] A. Sørensen et al. Nature **409**, 63 (2001).
 - [11] A. Sørensen, Phys. Rev. A **65**, 043610 (2002).
 - [12] A. Sinatra, Y. Castin, E. Witkovska, Phys. Rev. A **75**, 0033616 (2007); *ibid.*, Phys. Rev. A **80**, 033614 (2009).
 - [13] Yu. Kagan, B. V. Svistunov, and G. V. Shlyapnikov, Sov. Phys. JETP **75**, 387 (1992); Yu. Kagan and B. Svistunov, Phys. Rev. Lett. **79** 3331 (1997).
 - [14] K. Damle, S. N. Majumdar and S. Sachdev, Phys. Rev. A **54**, 5037 (1996).
 - [15] K. Góral, M. Gajda, K. Rzażewski, Opt. Express **8**, 92 (2001); D. Kadio, M. Gajda and K. Rzażewski, Phys. Rev. A **72**, 013607 (2005).
 - [16] M.J. Davis, S.A. Morgan and K. Burnett, Phys. Rev. Lett. **87**, 160402 (2001).
 - [17] M. J. Steel et al., Phys. Rev. A **58**, 4824 (1998).
 - [18] A. Sinatra, C. Lobo, Y. Castin, Phys. Rev. Lett. **87**, 210404 (2001).
 - [19] Yun Li et al., Eur. Phys. J. B **68** 365 (2009).
 - [20] M. Egorov et al., arXiv:1012.3813.
 - [21] A. Sinatra, Y. Castin, Phys. Rev. A **78**, 053615 (2008).
 - [22] Y. Castin, R. Dum, Phys. Rev. A **57**, 3008 (1998).
 - [23] We checked numerically that the approximation of replacing N_a, N_b by their average $N/2$ in the definition of the Bogoliubov modes is excellent for the timescales we are interested in.
 - [24] M. Lewenstein, Li You, Phys. Rev. Lett. **77** 3489 (1997); Y. Castin, J. Dalibard, Phys. Rev. A **55**, 4330 (1997).
 - [25] Y. Li, Y. Castin, and A. Sinatra, Phys. Rev. Lett. **100**, 210401 (2008).